ARL-RP-0563 ● DEC 2015

US Army Research Laboratory

Processing and Characterization of Needled Carbon Composites

by Bradley D Lawrence, Travis A Bogetti, and Ryan P Emerson

Reprinted from Proceedings of the 2015 Composites and Advanced Materials Expo (CAMX); 2015 Oct 26–29; Dallas, TX. Arlington (VA): CAMX Publishing; 2015. ISBN: 978-1-934551-20-2.

NOTICES

Disclaimers

ARL-RP-0563 ● DEC 2015

US Army Research Laboratory

Processing and Characterization of Needled Carbon Composites

by Bradley D Lawrence
TKC Global, LLC; Herndon, VA

Travis A Bogetti
Weapons and Materials Research Directorate, ARL

Ryan P Emerson
PPG Fiber Glass S&T Center; Shelby, NC

Reprinted from Proceedings of the 2015 Composites and Advanced Materials Expo (CAMX); 2015 Oct 26–29; Dallas, TX. Arlington (VA): CAMX Publishing; 2015. ISBN: 978-1-934551-20-2.

REPORT DOCUMENTATION PAGE	*Form Approved* *OMB No. 0704-0188*

1. REPORT DATE *(DD-MM-YYYY)*	**2. REPORT TYPE**	**3. DATES COVERED (From - To)**
December 2015	Reprint	December 2014–September 2015

4. TITLE AND SUBTITLE	**5a. CONTRACT NUMBER**
Processing and Characterization of Needled Carbon Composites	
	5b. GRANT NUMBER
	5c. PROGRAM ELEMENT NUMBER
6. AUTHOR(S)	**5d. PROJECT NUMBER**
Bradley D Lawrence, Travis A Bogetti, and Ryan P Emerson	
	5e. TASK NUMBER
	5f. WORK UNIT NUMBER
7. PERFORMING ORGANIZATION NAME(S) AND ADDRESS(ES)	**8. PERFORMING ORGANIZATION REPORT NUMBER**
US Army Research Laboratory ATTN: RDRL-WMM-A Aberdeen Proving Ground, MD 21005-5066	ARL-RP-0563
9. SPONSORING/MONITORING AGENCY NAME(S) AND ADDRESS(ES)	**10. SPONSOR/MONITOR'S ACRONYM(S)**
	11. SPONSOR/MONITOR'S REPORT NUMBER(S)

12. DISTRIBUTION/AVAILABILITY STATEMENT

Approved for public release; distribution is unlimited.

13. SUPPLEMENTARY NOTES

Reprinted from Proceedings of the 2015 Composites and Advanced Materials Expo (CAMX); 2015 Oct 26–29; Dallas, TX. Arlington (VA): CAMX Publishing; 2015. ISBN: 978-1-934551-20-2.

14. ABSTRACT

Needled carbon fiber composite materials are being investigated by the U.S. Army Research Laboratory (ARL) with the intent of reducing the sacrifices of in-plane properties typically associated with through-thickness reinforcement techniques such as Z-pinning, stitching, and tufting. This knockdown in strength is usually the result of different factors such as waviness in the fibers induced by the z-reinforcement, lowered fiber volume fractions due to swelling of the material, and physical damage to the carbon fibers themselves. Reductions in tensile strength of up to 25% for stitched carbon/epoxy composites have been reported, as have drops in elastic modulus of up to 15%. To investigate needled composite materials and overcome these issues, ARL has developed a unique in-house needle-processing capability which uses commercially-available felting needles to insert z-fibers into composite laminates at different angles (±45/90°) relative to the laminate plane. Previous work with needled glass/epoxy composites has shown a 270% improvement in Mode I interlaminar fracture toughness when needled at 90° to the laminate plane and significant increases in shear strength when needled at ±45°. In the current work, we characterize needled carbon/epoxy laminates via mechanical testing and x-ray micro-computed tomography (MicroCT) analysis. Needle wear issues associated with the carbon materials are addressed. Tensile strength of the needled carbon laminates was found to decrease minimally at low perforation densities but was reduced up to 11.5% at a high perforation density (75 perforations/cm2). Both compression strength and low velocity impact-induced delamination were found to be relatively unaffected by the needling process – even over the broad range of perforation densities investigated. Compression after impact (CAI) strength, however, increased significantly (18%) for a TTR reinforcement perforation density of 85 perforations/cm2 oriented at 90° and ±45° relative to the laminate plane.

15. SUBJECT TERMS

composite, material, needling, characterization, processing, carbon, laminate, epoxy, VARTM, through-thickness reinforcement, TTR, stitching, tufting, felting, z-pinning

16. SECURITY CLASSIFICATION OF:			**17. LIMITATION OF ABSTRACT**	**18. NUMBER OF PAGES**	**19a. NAME OF RESPONSIBLE PERSON**
					Bradley D Lawrence
a. REPORT	**b. ABSTRACT**	**c. THIS PAGE**			**19b. TELEPHONE NUMBER (Include area code)**
Unclassified	Unclassified	Unclassified	UU	22	410-306-4943

Standard Form 298 (Rev. 8/98)
Prescribed by ANSI Std. Z39.18

PROCESSING AND CHARACTERIZATION OF NEEDLED CARBON COMPOSITES

Bradley D. Lawrence
TKC Global LLC
13873 Park Center Road, Suite 400 North
Herndon, VA 20171

Travis A. Bogetti
U.S. Army Research Laboratory
4600 Deer Creek Loop
Aberdeen Proving Ground, MD 21005

Ryan P. Emerson
PPG Fiber Glass S&T Center
940 Washburn Switch Road
Shelby, NC 28150

ABSTRACT

Needled carbon fiber composite materials are being investigated by the U.S. Army Research Laboratory (ARL) with the intent of reducing the sacrifices of in-plane properties typically associated with through-thickness reinforcement techniques such as Z-pinning, stitching, and tufting. This knockdown in strength is usually the result of different factors such as waviness in the fibers induced by the z-reinforcement, lowered fiber volume fractions due to swelling of the material, and physical damage to the carbon fibers themselves [1]. Reductions in tensile strength of up to 25% for stitched carbon/epoxy composites have been reported, as have drops in elastic modulus of up to 15% [2]. To investigate needled composite materials and overcome these issues, ARL has developed a unique in-house needle-processing capability which uses commercially-available felting needles to insert z-fibers into composite laminates at different angles (±45/90°) relative to the laminate plane. Previous work with needled glass/epoxy composites has shown a 270% improvement in Mode I interlaminar fracture toughness when needled at 90° to the laminate plane and significant increases in shear strength when needled at ±45° [3]. In the current work, we characterize needled carbon/epoxy laminates via mechanical testing and x-ray micro-computed tomography (MicroCT) analysis. Needle wear issues associated with the carbon materials are addressed. Tensile strength of the needled carbon laminates was found to decrease minimally at low perforation densities but was reduced up to 11.5% at a high perforation density (75 perforations/cm^2). Both compression strength and low velocity impact-induced delamination were found to be relatively unaffected by the needling process – even over the broad range of perforation densities investigated. Compression after impact (CAI) strength, however, increased significantly (18%) for a TTR reinforcement perforation density of 85 perforations/cm^2 oriented at 90° and ±45° relative to the laminate plane.
The research reported in this document was performed in connection with contract/instrument W911QX-14-C-0016 with the U.S. Army Research Laboratory. The views and conclusions contained in this document are those of the authors and should not be interpreted as presenting the official policies or position, either expressed or implied, of the U.S. Army Research

1. INTRODUCTION

1.1 Background and Motivation

A wide variety of methods are described in the literature for improving the delamination resistance of laminated composite materials through the use of through-thickness-reinforcement (TTR); Z-pinning, stitching, and tufting. Z-pinning is a technique where small diameter pre-cured composite fiber or metal ”pins” are inserted orthogonally into the laminate, prior to cure, usually with the aid of ultrasonic vibration [1, 4-7]. Stitching of laminates involves the sewing of high strength yarns (e.g., glass, carbon, Kevlar) through an uncured assembly of plies [2, 8]. Tufting is a method by which a needle is used to insert high strength yarns (i.e., threads) through the dry fabric or prepreg laminate, leaving a loose thread loop underneath [9-11]. Stitching is more complex than tufting and involves interlocking of orthogonally placed reinforcing yarns to hold plies together. While each method is unique - all rely on fiber reinforcement, placed in the normal direction of the laminate, to prevent or inhibit the plies from separating (i.e., improving delamination resistance). This area of research has long been of great interest to the composites community where delamination resistance is the primary driver in structural design considerations (i.e., improved damage tolerance and durability). The myriad of material combinations, applications, geometries and load spectra preclude conclusive statements on which of these is the best TTR technology, but typically the benefits carry trade-offs in manufacturability, degradation of in-plane strength, and cost [12].

1.2 Needling Research

Another effective method for achieving 3D reinforcement is needling (i.e., needle-punching) [13-16]. In this process, the 3D reinforcement is created with downward-barbed needles that push TTR into an otherwise 2D laminate. As such, needling is similar to stitching or tufting but with one important difference: the needling process typically inserts 20-60 through-thickness filaments at each penetration site, whereas the threads used in tufting and stitching usually contain several thousands of filaments. This is significant because in-plane fiber distortion caused by the tuft/stitch thread is identified in the literature as the primary cause for the typically reported 5-15% reduction in the in-plane stiffness and strength [9, 10]. Needled through-thickness reinforcement has the potential to offer less reduction of in-plane strength because the fiber distortions are significantly reduced.

Needling was briefly evaluated as a 3D reinforcement method for structural composites under the Survivable, Affordable, Repairable Airframe Program [12]. Several examples are found in the literature of needled/felted carbon-carbon (C/C) composites for high temperature applications such as ablative aerospace heat shields [11] and automobile brake pads [15]. The needled TTR described in these reports was created by plunging downward-barbed needles through dry laminates of carbon fiber prior to pyrolysis, essentially breaking some of the in-plane carbon fiber to orient a fraction of the filaments in the through-thickness direction. The flexural strengths of the resultant needled C/C materials were reported in the range of 100-130 MPa and, as such, these materials are not appropriate for high strength applications. Non-structural needled aramid fabric laminates are not uncommon and are commercially available as air filtration media and in personnel protection products [17].

With the exception of previous ARL research, the literature provides no examples of the needling process of laminated materials as described in the present report. Figure 1 provides an illustration of the fundamental components and process of the present application of needling. In this process, the downward-barbed needle grabs and inserts a so-called "supply" material into the 2-D laminate.

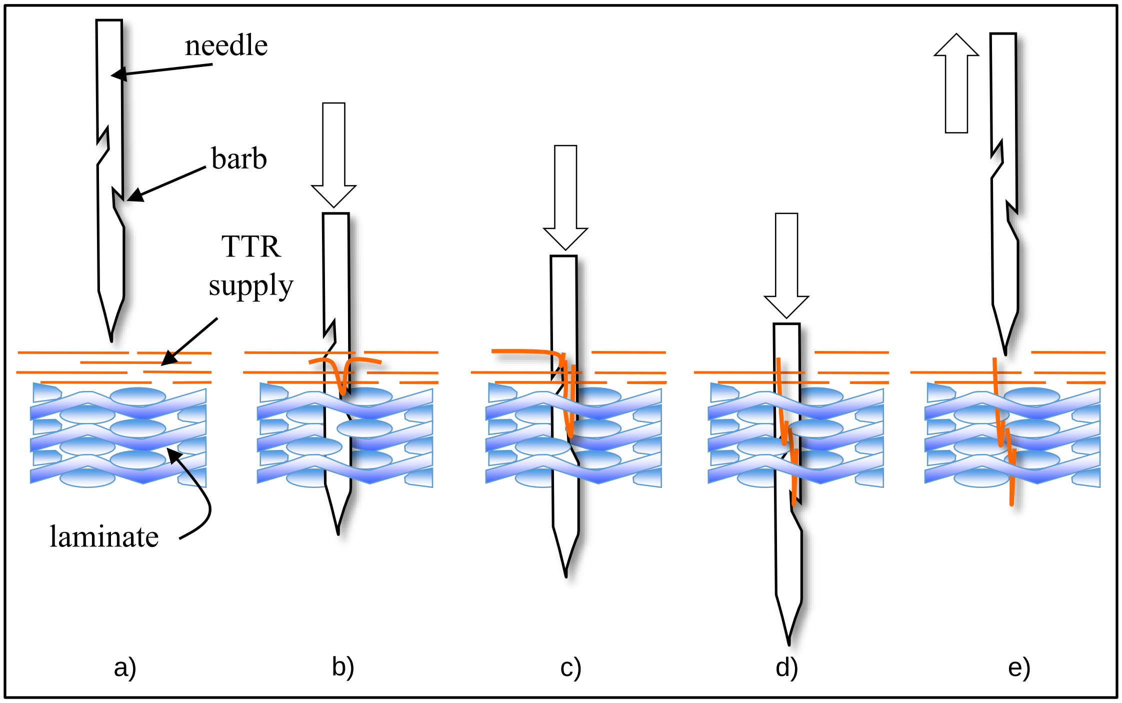

Figure 1. Illustration showing how the needle pushes supply material into the carrier material.

In a previously reported study [18], proof-of-concept trials were conducted at ARL with plain-weave S2-glass structural laminates reinforced with aramid filaments in the through-thickness direction using a unique needling process. Laminates were needled in dry form and subsequently infused and cured with epoxy resin using vacuum-assisted resin transfer molding (VARTM). The needling was performed using semi-automated processing equipment, commercial off-the-shelf needles and aramid random fiber matting designed for other applications. Needled laminates were tested under low velocity impact (LVI), compression after impact (CAI), in-plane compression, and 4-point bend. Needled specimens exhibited a 10-15% increase in effective stiffness (force-deflection response) under LVI, a 50% increase in CAI strength, a 9% increase in in-plane compressive strength and a 17% increase in flexural strength.

More recently, researchers at the ARL have automated the needling process described in [18], to include the ability to insert TTR reinforcement at ±45° relative to the laminate plane [3]. In their work, VARTM infused S2-glass/epoxy laminates, needle reinforced with aramid fibers, were characterized according to a variety of ASTM standard test methods. Dramatic improvements in

Mode I fracture toughness, in-plane compression strength, and interlaminar shear strength were observed - without a significant degradation of the in-plane tensile strength.

1.3 Current Investigation

This effort extends the needling work of [18] and [19] on glass fabric laminates to woven carbon fabric laminates. Here we describe additional process improvements and report characterization results for VARTM infused carbon fiber/epoxy laminates with aramid TTR reinforcement at perforation densities between 25 and 85 perforations/cm^2. Unlike the glass fabrics, excessive needle wear was found to be an issue with the carbon fabric materials. However, a tungsten coating applied to the needles was shown to significantly reduce barb erosion. Tensile strength of the needled carbon laminates was found to decrease only slightly for the lowest perforation density (25 perforations/cm^2) but was reduced up to 11.5% for the highest perforation density of 75 perforations/cm^2. Compression strength was found to be relatively unaffected by the needling process – even over the broad range of perforation densities investigated. Surprisingly, low velocity impact-induced delamination was also found to be relatively unaffected by the needled TTR reinforcement. The compression after impact (CAI) strength, however, increased significantly for the TTR reinforcement perforation density of 85 perforations/cm^2 oriented at ±45° relative to the laminate plane. The following sections detail the needling process and characterization methods used to assess the delamination resistance and structural performance of needled woven carbon fiber composite laminates.

2. MATERIALS AND PROCESSING

2.1 Materials

The fiber reinforcement used in this work is a T300 3K plain woven carbon fabric (193 g/m^2 per ply) [19]. Plies of aramid randomly-oriented short fiber mat (0.5 inch mean fiber length – 34 g/m^2 per ply) [20] were used as the TTR supply material, whose fibers are inserted into the laminate via the needling process. The supply material is placed on top of the plies of carbon fabric. All laminates in this work incorporate a [0/90] ply architecture and are infused with SC-15 rubber-toughened epoxy resin [21] using VARTM. All samples were cut using a water jet cutter.

2.2 Needling Process

All needled composites in this work were processed using a fully-automated needling facility that is centered on an *x*-*y*-*z* gantry custom-built at ARL with modular framing [22], shown in Figure 2. The gantry sits on top of a MIC6 aluminum base plate and is clamped to a laboratory table. The facility is currently capable of processing flat plates of dimensions as large as 900 × 1250 mm.

The three gantry axes move independently along rails and ball screws and are controlled by stepper motors and a motion-control kit that operates with G-code commands [23]. These commands drive the needling tool to coordinates in *x*-*y*-*z* space at pre-programmed velocities. Programs can be written which enable the tool to be moved in virtually any pattern desired by the operator. All aspects of the facility's operation are computer-controlled. Power to the tool is controlled by G-code commands via a relay, thus completing the facility's CNC (computer numerical control) automation. The hardware inside the needling tool converts the rotary motion of the motor to reciprocating motion (14.4 Hz) at the needles. The needles are held in place with three mounting blocks and plunge through a hole in the "foot" of the tool at three different angles as seen in Figure 3. The stroke length of the 90° needles is 25.4 mm and the stroke lengths of the +45° and -45° needles are 35.9 mm. In this way, the *z*-component of the stroke of each needle is equivalent.

The height of the tool relative to the table surface is adjustable to accommodate different thicknesses of material. This adjustment includes springs that counteract most of the weight of the tool to prevent it from dragging material around the surface of the table. The foot applies weight to the material, which compacts it slightly so it can be needled more effectively. The degree of material compaction can be changed by adjusting the tool's *z*-position. The height of the foot is adjustable relative to the tool in order to control the depth of needle penetration into the material. The tabletop incorporates plies of dry fabric material covered with a plastic sheet. This provides a firm backstop that is still permeable to the needles, allowing the TTR fibers to be inserted completely through the laminate without interference.

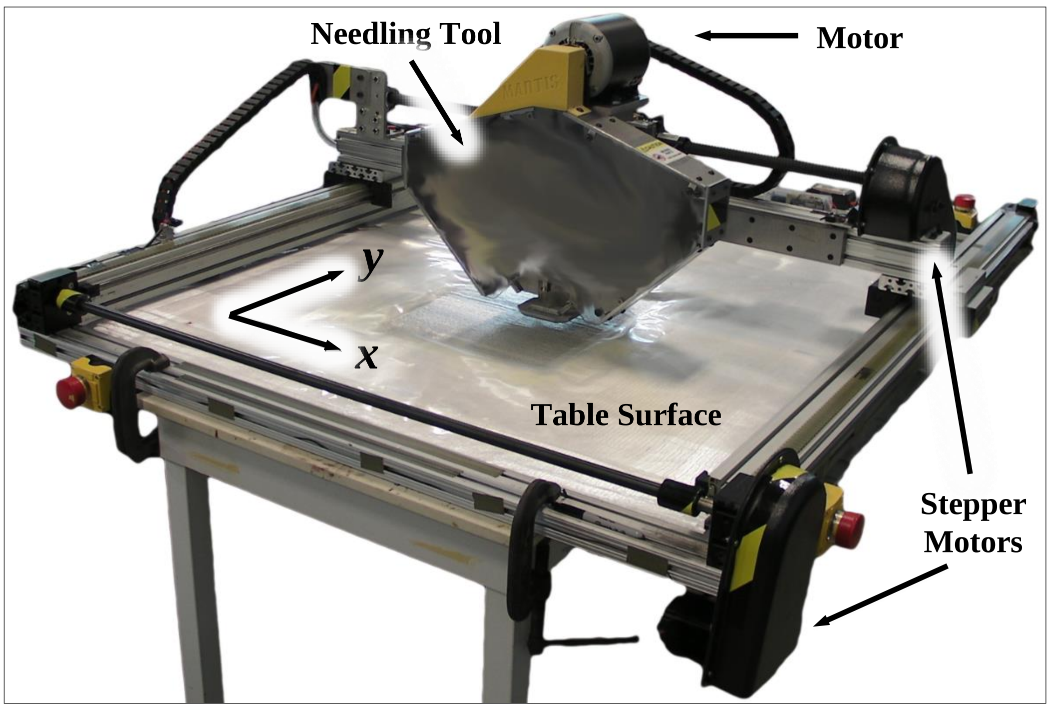

Figure 2. Photograph of ARL automated needling facility.

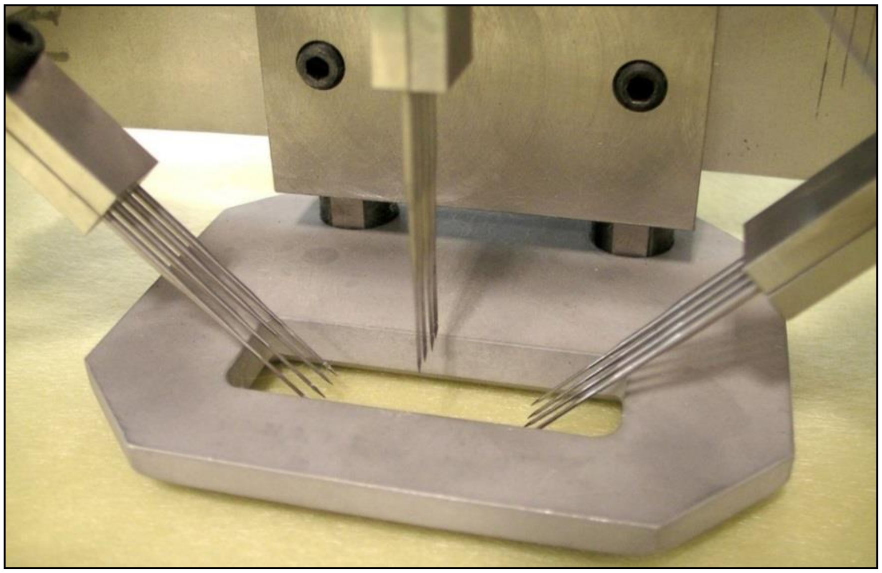

Figure 3. Needling foot with all needles installed.

Figure 4 is a photograph illustrating the physical geometry of a typical felting needle. The inset shows close-up images of the working parts of other types of commercially-available felting needles. The needles designated "611," "615", and "601" are products of Groz-Beckert [24]. The "C36" and "C36B" needles are products of the Colonial Needle Company [25]. The 611 "crown" needle is used in the present work. The cross-sections of all needle working parts shown are triangular, and there are barbs on the hidden apex of each needle with the exception of needle style 601, which has only a single barb on one apex.

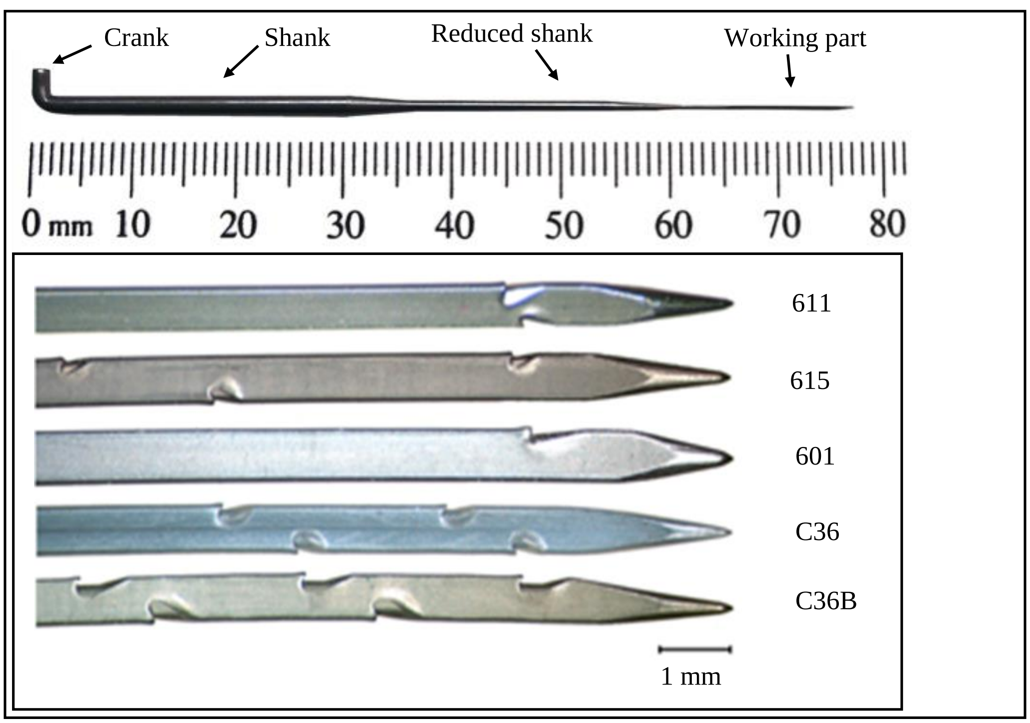

Figure 4. Examples of various commercially-available felting needles.

3. RESULTS AND DISCUSSION

3.1 Needled Microstructure

X-ray micro-computed tomography (MicroCT) was also used to interrogate the unique 3D microstructure resulting from the needling process. Figure 5 is a pair of MicroCT scans showing the needled architecture of a 4 mm diameter T300/SC-15 sample from the laminate side and top view perspectives. In the side view, local in-plane fiber tow distortion is visible at the needle penetration site, but the actual extent of any carbon fiber damage is not clearly evident. The top view illustrates how the TTR reinforcement is physically embedded in the woven carbon fiber tows. The actual size and influence of this needle affected region should be less than that associated with stitched or z-pinned TTR reinforcements, due to the inherently less intrusive nature of the needling process. However, a more quantitative assessment of how the needling process effects the local architectural is required and is part of our ongoing investigation.

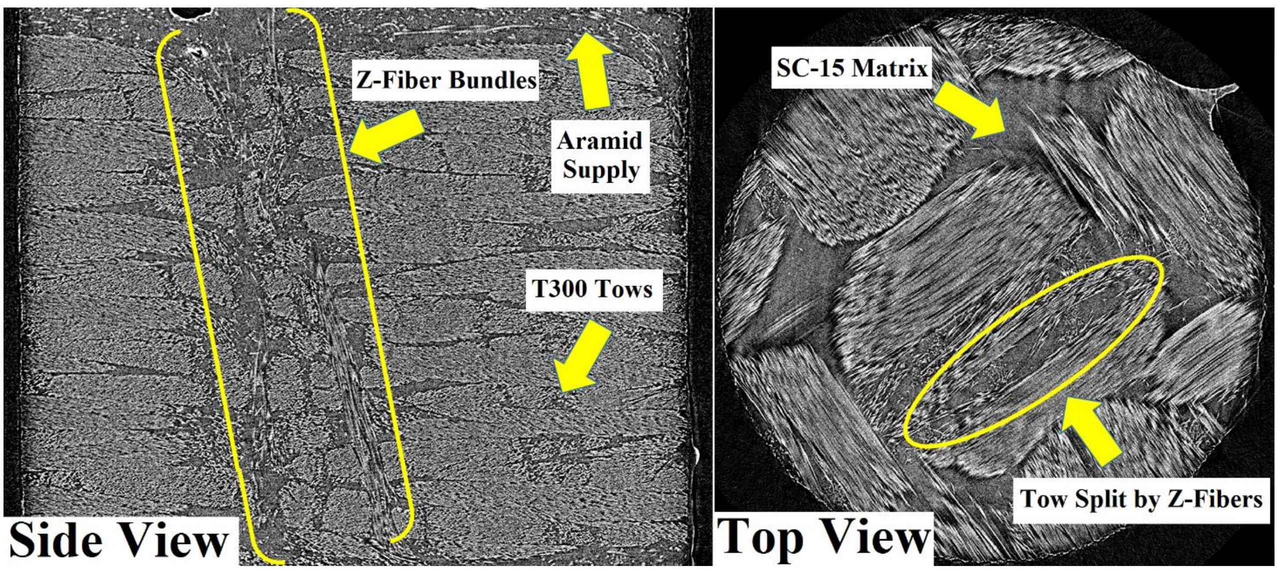

Figure 5. MicroCT of ARL-needled T300/SC-15 composite.

3.2 Needle Wear

Over time, felting needles normally experience wear which is dependent upon various factors such as the material being needled, the material from which the needle is manufactured, etc. The primary wear points of concern are the barbs, which slowly erode. As a barb wears, the efficiency with which it converts the supply material to TTR decreases, and it is eventually rendered incapable of grabbing any useful amount of new material with which to insert z-fibers into the laminate [26].

Previous ARL experimentation with needled S2 glass fiber laminates has shown a gradual rate of wear. Laminates were needle-processed at high perforation densities with needles experiencing over 100,000 perforations. In these cases, needle wear was slow enough that a given set of needles was still nominally usable even after the needling run was completed. Needling of carbon fiber laminates, however, is far more challenging with accelerated wear and increased occurrence of barb fracture. Needling through 193 g/m^2 T300 3K plain-woven fabric caused severe wear after only 50,000 perforations, leaving two out of the three barbs on a given needle unusable (Figure 6). The exact mechanism behind this increased needle wear is not completely understood or quantified.

To mitigate the erosive effects of the carbon fiber, options were explored for high-performance wear-resistant coatings. Tungsten was selected for its ease of application as well as the availability of an in-house sputter coating capability. A small exploratory batch of needles was coated, but the fixturing holding the needles in the specimen chamber broke shortly after the process began. Even with a truncated coating process, these needles showed reduced wear after 72,000 perforations through a T300 laminate, with the barbs remaining reasonably intact and still usable (Figure 6).

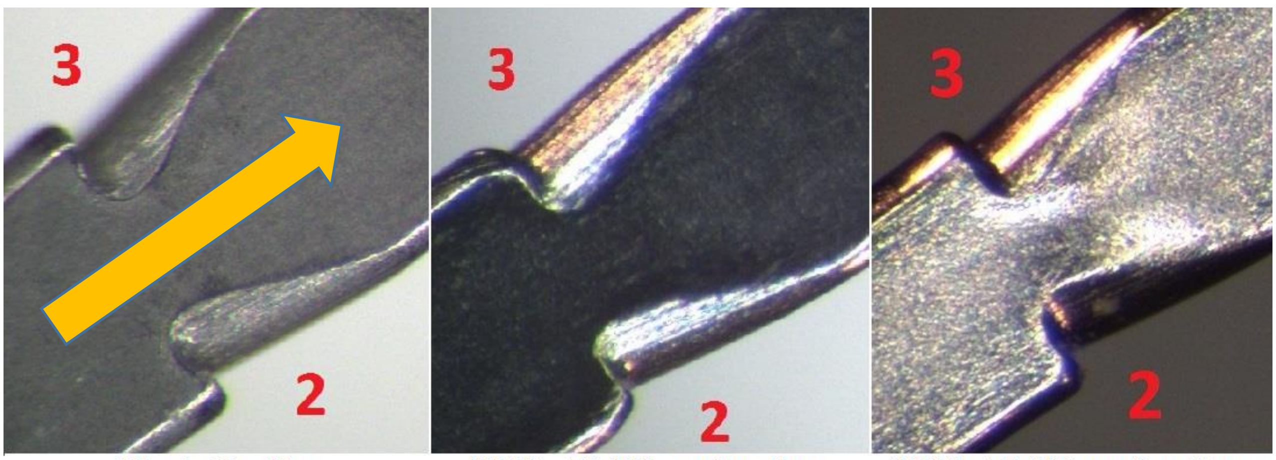

Figure 6. Comparison of virgin needle barbs with uncoated and tungsten-coated barbs used to needle carbon fabric.

3.3 Tensile Strength

To study the effects of needling on in-plane tensile strength, needled composites were manufactured and subjected to tension testing. Laminates were constructed from 12 plies of T300 with three plies of aramid supply material. Needled samples were needle-processed at 90°, orthogonal to the laminate plane. Non-needled control samples were also manufactured.

Samples were tested in accordance with the ASTM standard test method for tension [27] on an Instron 5985 load frame equipped with hydraulic grips [28]. The peak tensile stress decreases by 1.2% at a low perforation density (25 perforations/cm^2) but drops noticeably as the perforation density increases. This is most likely the result of damage done to the fibers by the needle barbs, as well as possible disturbance of fiber linearity. A reduction in peak tensile strength of 11.5% is observed for samples needled at 75 perforations/cm^2 (Figure 7). Test results and relevant statistics are summarized in Table 1.

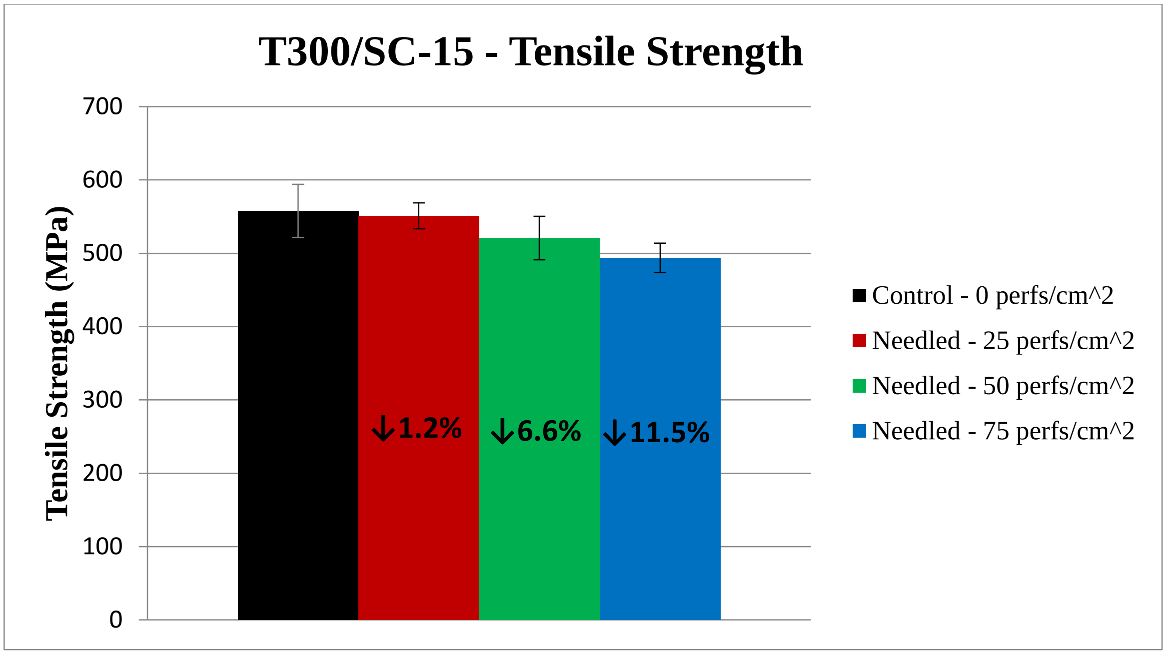

Figure 7. Comparison of tensile strengths.

Table 1. Summary of tensile strengths.

Condition	Average Max Stress (MPa)	STDEV	Change vs. Control (%)
Control - 0 perfs/cm^2	557.9	36.3	---
Needled - 25 perfs/cm^2	551.1	17.7	-1.2
Needled - 50 perfs/cm^2	520.8	29.7	-6.6
Needled - 75 perfs/cm^2	493.6	20.1	-11.5

3.4 CLC Compression Strength

Compression testing was conducted on an Instron 1127 load frame using a CLC (Combined Loading Compression) fixture. Testing followed parameters defined by the ASTM standard for this type of test [29]. Samples were made from 16 plies of T300 with three plies of aramid supply material. Needled samples were needle-processed at 90°. All samples had their ends machined to maximize parallelism between loading surfaces.

Needle processing did not cause any significant improvement or reduction in the material's compression strength. Figure 8 compares the compression strengths observed for each processing condition. A 6.6% decrease is seen at 25 perforations/cm^2, but very little change occurs at 50 and 75 perforations/cm^2. Peak compressive stress results with statistics are shown in Table 2. The gage section failures of the CLC specimens are detailed in Figure 9. The overall failure mode appears to be affected by increasing perforation density, progressing from a buckling failure to a brooming type of failure. This may be a result of the TTR fibers tying the material together. However, needling does not appear to have visibly confined or influenced the propagation of delamination damage. Samples needled at 50 and 75 perforations/cm^2 were more likely to break in two at failure.

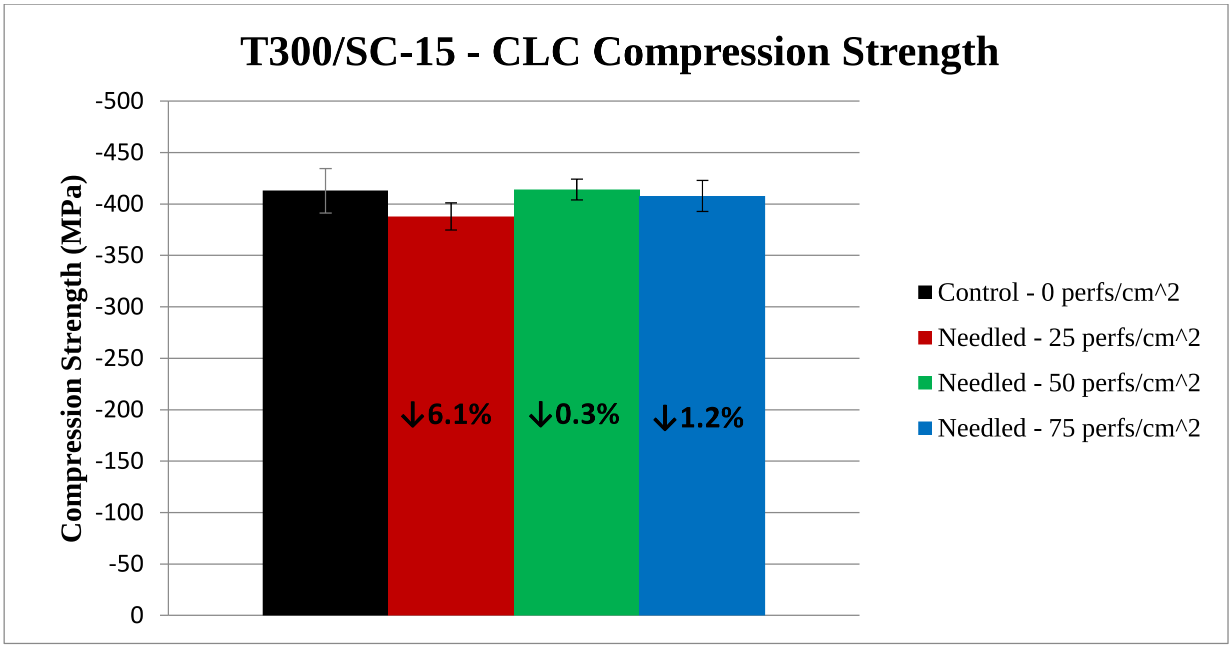

Figure 8. Comparison of compression strengths.

Table 2. Summary of compression strengths.

Condition	Average Max Stress (MPa)	STDEV	Change vs. Control (%)
Control - 0 perfs/cm^2	-412.9	21.6	---
Needled - 25 perfs/cm^2	-387.9	13.2	-6.1
Needled - 50 perfs/cm^2	-414.1	10.1	0.3
Needled - 75 perfs/cm^2	-407.8	15.1	-1.2

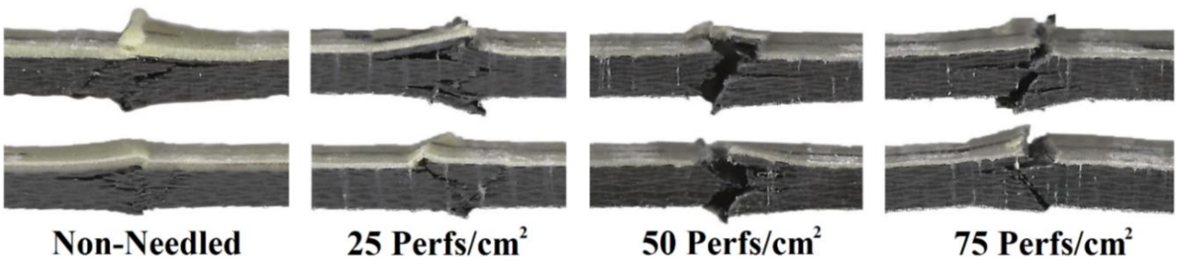

Figure 9. Failure detail of carbon specimens subjected to CLC compression testing.

3.5 Low Velocity Impact Response

To evaluate material impact damage tolerance, needled and non-needled samples were subjected to LVI testing [30]. 16 plies of T300 were laid up with three plies of aramid supply. Laminates were needle-processed at five directions relative to the XY laminate plane: 90°, ± 45° in the X-direction, and ± 45° in the Y-direction. Needling at 45° angles is intended to improve the laminate's resistance to interlaminar shear.

An overlay of all LVI force-displacement histories is shown in Figure 10. Few differences are apparent between needled and non-needled impacts, except for a possible slight increase in the initial stiffness in the 1.5 to 3 mm range of the loading portion of the curve. Overall, the impact response of this material system does not appear to be significantly affected by needle-processing. Maximum force and displacement are summarized in Table 3. Needling decreased the average peak force value by 2.6%, while peak displacement decreased by 0.5%.

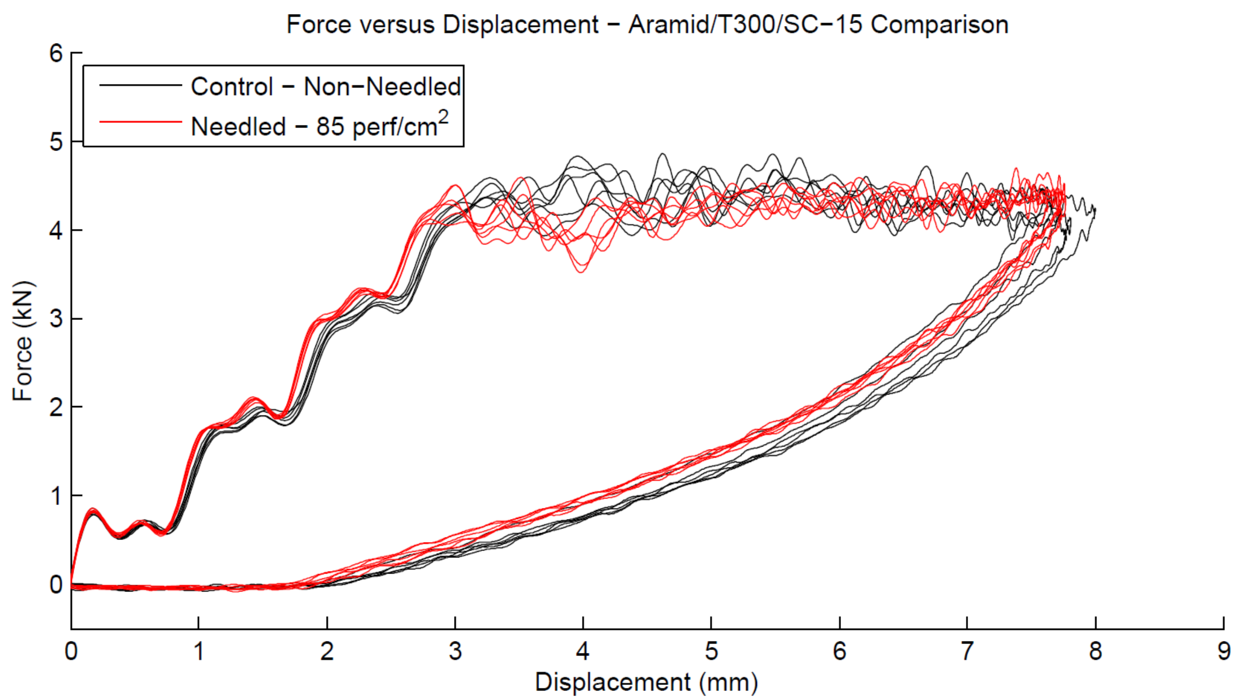

Figure 10. Force vs. displacement history showing low-velocity impact response.

Table 3. Summary of maximum force and displacement of carbon composites under low-velocity impact.

Condition	**F_{max} (kN)**	**STDEV**	**Change vs. Control (%)**	**$disp_{max}$ (mm)**	**STDEV**	**Change vs. Control (%)**
Control - 0 Perfs/cm^2	4.7	0.1	---	7.8	0.1	---
Needled - 85 Perfs/cm^2 at 90/±45°	4.6	0.1	-2.6	7.7	0.1	-0.5

3.6 Non-Destructive Evaluation

To quantify the extent of damage caused by LVI, samples were non-destructively evaluated using through-transmission C-scans. Samples were scanned pre- and post-impact to track the progression of damage resulting from impact testing. C-scans were analyzed using ImageJ software [31] to quantify the total damage area present. A 1.4% decrease in total damage area was observed in the needled samples (Figure 11). A slight difference in the general shape of the damage zones between the two processing conditions is seen in Figure 12. This could possibly indicate that the z-fiber bundles are changing the way the impact energy is dissipated in the material, restricting damage from propagating locally and forcing it to travel a longer distance along the primary tows. Damage area results are summarized in Table 4.

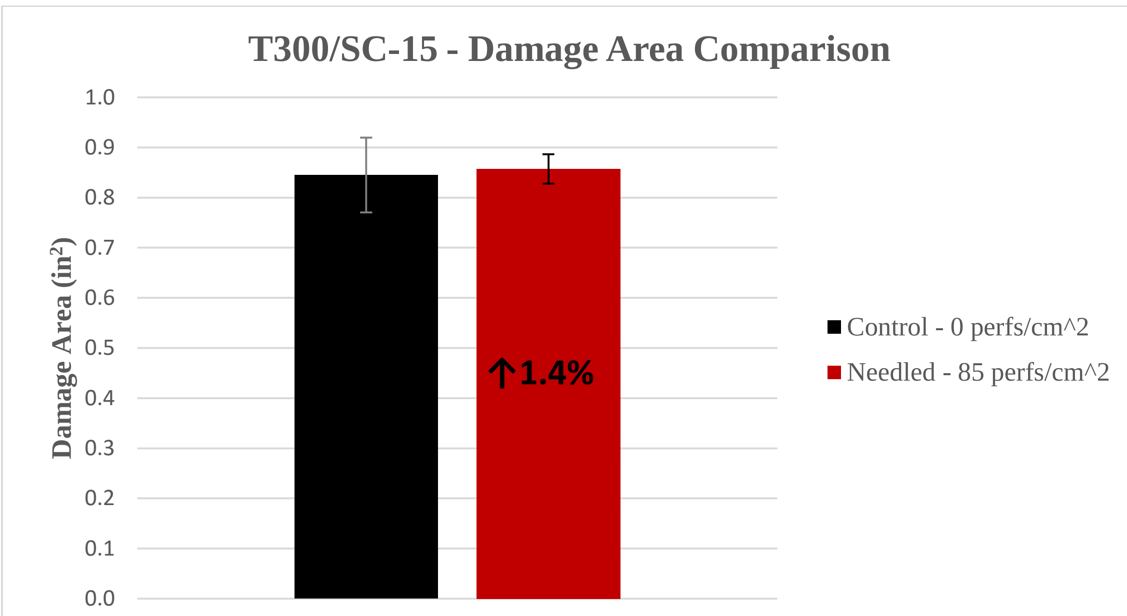

Figure 11. Comparison of low-velocity impact damage areas.

Table 4. Summary of damage areas resulting from low-velocity impact.

Condition	Average Damage Area (in^2)	STDEV	Change vs. Control (%)
Control – 0 perfs/cm^2	0.85	0.07	---
Needled - 85 Perf/cm^2 at 90/±45°	0.86	0.03	1.4

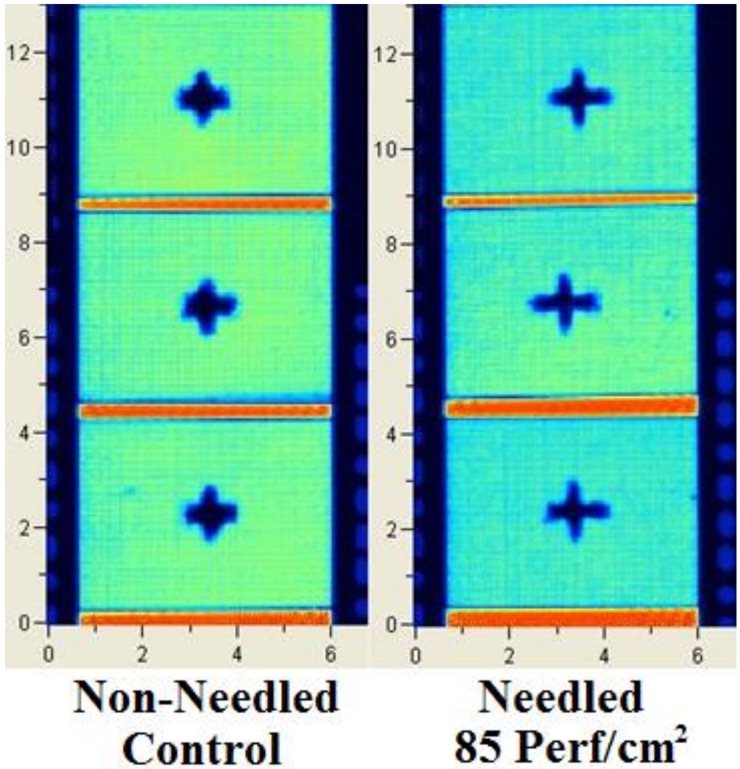

Figure 12. C-scan images of carbon fiber composites subjected to low-velocity impact.

3.7 Compression After Impact Response

After being subjected to LVI, samples underwent CAI testing [32] to determine their ultimate residual compressive strength. Figure 13 compares the residual compressive strengths of needled and non-needled samples. The needled samples show a remarkable 18% improvement in residual compressive strength versus the non-needled control. This is most likely due to the presence of ±45° TTR, which provides local buckling stability for the individual layers of damaged fabric. The tendency of the impact damage to propagate along the primary tows instead of the surrounding material is also a possible reason for the increase in compression strength (Figure 12). CAI results are summarized in Table 5.

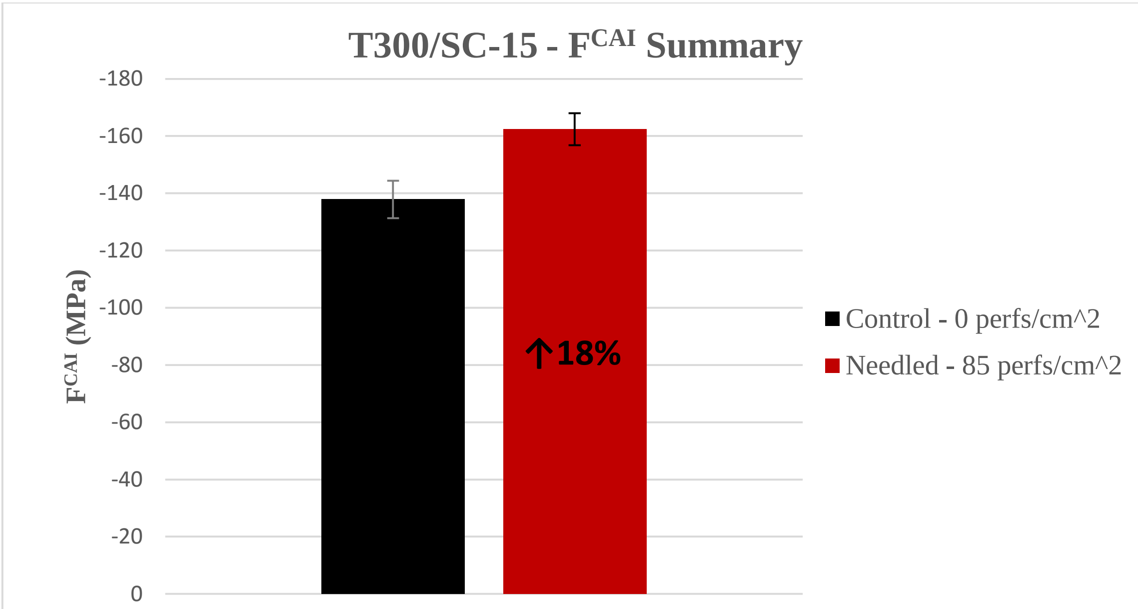

Figure 13. Comparison of compression after impact ultimate residual compressive strength.

Table 5. Summary of compression after impact ultimate residual compressive strength.

Condition	Avg. F^{CAI} (MPa)	STDEV	Change vs. Control (%)
Control - 0 perfs/cm^2	-137.9	6.6	---
Needled - 85 perfs/cm^2	-162.4	5.6	18

4. CONCLUSIONS

4.1 Effects on Material Strength

In this work, needle-processing was shown to have varied effects on the mechanical properties of carbon fiber/epoxy laminates. Tensile strength was reduced by 1.2% to 11.5% with increasing perforations orthogonal to the laminate plane. Compression strength was only slightly affected, being reduced by 6.1% at 25 perforations/cm^2, but only falling by 0.3% and 1.2% at 50 and 75 perforations/cm^2, respectively. Low-velocity impact testing showed only a slightly different response between the materials, with samples needled at multiple angles experiencing a 2.6% lower peak load with and 0.5% difference in peak displacement. The most encouraging finding was that needle-processing was shown to enhance the compression after impact ultimate residual compressive strength of the carbon fabric/epoxy laminates by 18% at 85 perforations/cm^2.

4.2 Effects on Delamination/Damage Propagation

Multi-angle needle processing was found to have very little effect on total damage area resulting from low-velocity impact. Analysis of C-scan images showed a 1.4% increase in total damage area for needled samples. The damage areas for needled and non-needled samples varied slightly, indicating a possible alteration of the failure mechanism and/or energy dissipation characteristics resulting from the placement of the needled z-fiber architecture. CLC compression samples also showed different failure characteristics, with higher perforation densities appearing to confine damage and reduce the occurrence of buckling failures.

4.3 Future Work

This work represents a preliminary investigation into needled carbon composites, and many opportunities exist for further study. Aramid is the only TTR supply material investigated thus far, and a multitude of different supply materials exist which could possibly be used. In the interest of further expanding the applications of this emerging technology, there is a great interest in developing the capability to needle prepregs. LVI and CAI testing of samples needled at 90° and ±45° would enable researchers to quantify the influence of differently-angled TTR fibers on material strength and durability. LVI and CAI data for materials needled at 90° would also be more readily compared to the tension and compression results already presented. Expanded exploration of wear-resistant coatings for needles would also be of great benefit.

5. REFERENCES

1. Mouritz, A.P.; "Review of Z-Pinned Composite Laminates." *Composites: Part A* 38 (2007): 2383-2397

2. Larsson, F.; "Damage Tolerance of a Stitched Carbon/Epoxy Laminate." *Composites: Part A* 28 (1997): 923–934.

3. Emerson, R.P.; Lawrence, B.D.; Montgomery, A.; Safriet, S.; "Improvements to the Processing and Characterization of Needled Composite Laminates." *Proceedings of the American Society for Composites 28th Annual Technical Conference* State College, Pennsylvania, September 9-11, 2013.

4. Cartié, D.D.R., Laffaille, J-M., Partridge, I.K. Brunner, A. "Fatigue Delamination Behavior of Unidirectional Carbon Fibre/Epoxy Laminates Reinforced by Z-fiber Pinning." *Engineering Fracture Mechanics* 76 (2009): 2834–2845.

5. Cartié, Denis D.R.; Dell'Anno, Giuseppe; Poulin, Emilie; Partridge, Ivana K.; "3D Reinforcement of Stiffener-to-Skin T-Joints by Z-Pinning and Tufting," *Engineering Fracture Mechanics* 73 (2006): 2532-2540.

6. Partridge, I.K., Cartié, D.D.R. "Delamination Resistant Laminates by Z-fiber® Pinning Part I: Manufacture and Fracture Performance." *Composites: Part A* 36 (2005): 55–64.

7. Grassi, M., Zhang, X., Meo, M. "Prediction of Stiffness and Stresses in Z-fibre Reinforced Composite Laminates." *Composites: Part A* 33 (2002): 1653-1664.

8. Mouritz, A.P., Leong, K.H., and Herszberg, I., "A Review of the Effect of Stitching on the In-Plane Mechanical Properties of Fibre-Reinforced Polymer Composites," *Composites: Part A* 28A (1997): 979-991.

9. De Verdiere, M.C., Pickett, A.K., Skordos, A.A., Witzel., V. “Evaluation of the Mechanical and Damage Behaviour of Tufted Non Crimped Fabric Composites Using Full Field Measurements.” *Composites Science and Technology* 69 (2009): 131-138.

10. G. Dell’Anno et al, “Exploring Mechanical Property Balance in Tufted Carbon Fabric/Epoxy Composites,” *Composites Part A* 38 (2007): 2366-2373.

11. Pierson, H.O., Northrop, D.A. “Carbon-Felt, Carbon-Matrix Composites: Dependence of Thermal and Mechanical Properties on Fiber Precursor and Matrix Structure,” *Journal of Composite Materials* 9 (1975): 118-137.

12. Wilson, H., Minguet, P., Schaff, J., Townsend, W., and Davis, T., “Survivable, Affordable Reparable Airframe Program (SARAP) Technology Maturation and Trade Studies Structures Technology Final Report (Limited Distribution),” RDECOM TR06-D-10, 2005.

13. Bradley, L.R., Bowen, C.R., McEnaney, B., Johnson, D.C. “Shear Properties of a Carbon/Carbon Composite with Non-Woven Felt and Continuous Fibre Reinforcement Layers.” *Carbon* 45 (2007): 2178–2187.

14. Zhang, X., Hejun, L., Hao, Z., Cui, H. “Effect of Needling Parameters on Mechanical Properties of C/C Composites Reinforced by Carbon Cloth.” *Materials Science Forum* 546-549 (2007): 1521-1524.

15. Han, C.L., Zhao, D.L., Zhang, L., Shyen. Z.M. “Microstructure and Mechanical Property of Three-Dimensional Needled C/SiC Composites Prepared by Precursor Pyrolysis,” *Key Engineering Materials* 434-435 (2010): 45-47.

16. A-lin, J., Hong, C., He-jun, L., Wen, C., Ling-ling, J. “Performance Analysis of a Carbon Cloth/Felt Layer Needled Preform.” *New Carbon Materials* 26(2) (2011): 109–116.

17. Tex Tech Industries, Portland, Maine.

18. Emerson, R., Cain, J., Simeoni, M., Lawrence, B. “Processing and Evaluation of 3D Reinforced Needled Composite Laminates.” *ARL-TR-6107*; U.S. Army Research Laboratory: Aberdeen Proving Ground, Maryland, September 2012.

19. Toray Carbon Fibers America, Flower Mound, TX.

20. Technical Fibre Products Inc., Schenectady, NY.

21. Applied Poleramic Inc., Benicia, California.

22. 80/20 Inc., Columbia City, Indiana.

23. Automation Technology Inc., Hoffman Estates, Illinois.

24. Groz-Beckert USA Inc., Charlotte, North Carolina.

25. Colonial Needle Company, White Plains, New York.

26. Foster Needle Company, Inc., Manitowoc, Wisconsin.

27. ASTM Standard D 3039M-08, 2008, "Standard Test Method for Tensile Properties of Polymer Matrix Composite Materials" ASTM International, West Conshohocken, PA, 2008.

28. Instron, Norwood, MA.

29. ASTM Standard D 6641M-09, 2009, "Standard Test Method for Compressive Properties of Polymer Matrix Composite Materials Using a Combined Loading Compression (CLC) Test Fixture," ASTM International, West Conshohocken, PA, 2009.

30. ASTM Standard D 7136M-12, 2012, "Standard Test Method for Measuring the Damage Resistance of a Fiber-Reinforced Polymer Matrix Composite to a Drop-Weight Impact Event," ASTM International, West Conshohocken, PA, 2012.

31. ImageJ Software, National Institutes of Health, Bethesda, Maryland.

32. ASTM Standard D 7137M-12, 2012, "Standard Test Method for Compressive Residual Strength Properties of Damaged Polymer Matrix Composite Plates," ASTM International, West Conshohocken, PA, 2012.

1 DEFENSE TECHNICAL
(PDF) INFORMATION CTR
DTIC OCA

2 DIRECTOR
(PDF) US ARMY RESEARCH LAB
RDRL CIO LL
IMAL HRA MAIL & RECORDS
MGMT

1 GOVT PRINTG OFC
(PDF) A MALHOTRA

2 DIR USARL
(PDF) RDRL WMM A
B LAWRENCE
T BOGETTI